THE JOURNAL OF PHYSICAL CHEMISTRY C
A JOURNAL OF THE AMERICAN CHEMICAL SOCIETY

pubs.acs.org/JPCC

Article

# Impact of Hydration on Supported $V_2O_5/TiO_2$ Catalysts as Explored by Magnetic Resonance Spectroscopy

Nicholas R. Jaegers, Yong Wang,* Jian Zhi Hu,* and Israel E. Wachs*

Cite This: *J. Phys. Chem. C* 2021, 125, 16766–16775

Read Online

ACCESS | Metrics & More | Article Recommendations | Supporting Information

**ABSTRACT:** Supported vanadium oxide catalysts are important industrial materials for a wide array of chemical transformations. The condition of surface hydration is of particular interest as a reflection of the state of freshly manufactured catalysts prior to their activation in catalytic reactors or under the conditions of photocatalysis where surface vanadia are exposed to moisture. Under such conditions, the surface vanadia species undergo structural changes, as evidenced by $^{51}V$ magic-angle spinning nuclear magnetic resonance ($^{51}V$ MAS NMR) in this study. For low surface vanadia densities on titania, a modest trend toward the formation of dimeric and oligomeric vanadia species was observed under hydrated conditions when compared to the corresponding dehydrated catalyst, which contains a large abundance of monomeric vanadia species. The incorporation of tungsten oxide into the $V_2O_5/TiO_2$ catalyst with low surface vanadia density, however, is found to better stabilize the surface vanadia species on the titania support upon hydration than its tungsta-free counterpart. This stabilization is not an intrinsic property of more extensively oligomerized surface vanadia species in the presence of tungsten oxide, which is evidenced by the conditions of high concentrations of surface vanadia oligomers on titania that exhibit dramatic structural changes upon hydration. At high surface vanadia coverage under hydrated environments, the simultaneous observation of polycrystalline $V_2O_5$ nanoparticles and a mobile phase of surface vanadia species is apparent, where vanadia species are dissolved in a thin hydration layer on the titania support. These new findings have broad implications on the behavior of other metal-oxide species on high surface oxide supports under hydrated conditions.

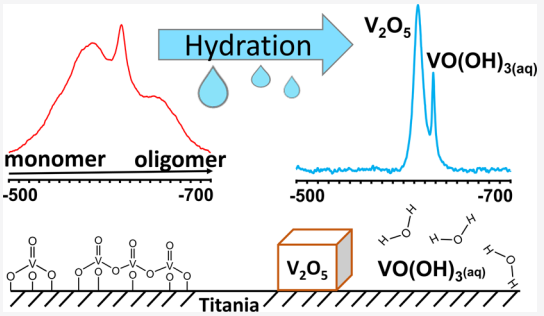


## INTRODUCTION

Vanadium oxide-based materials are important industrial catalysts employed in myriad applications. Vanadium oxide in catalytic applications is typically present as a minority phase supported atop another oxide material (the support) with a high surface area, and it has shown effectiveness in chemical conversions ranging from oxidative dehydrogenation (ODH) of alkanes and alcohols,[1,2] $SO_2$ oxidation,[3] *o*-xylene oxidation,[4] selective catalytic reduction (SCR) of nitrogen oxides,[5] and photocatalytic conversion of alcohols.[6] In its pentavalent state, surface vanadia species that favorably catalyze photo/thermochemical conversion occupy structural and coordinative configurations dissimilar to their bulk polycrystalline $V_2O_5$ molecular structure. This structural contrast imbues alternative reactive properties that are dependent on specific molecular arrangements. Factors such as the supporting oxide, vanadia loading, and chemical environment of the material intimately affect the supported vanadia species that are present.[7] For example, vanadia structures are described to evolve from monomeric species (distorted $VO_4$ centers with one V═O and three V−O-support bonds) at low surface density to oligomeric species at moderate loadings and finally to the bulk polycrystalline $V_2O_5$ nanoparticles above monolayer coverage.[8,9] As such, there exists a desire to characterize these materials under the different environments they encounter.

Efforts to understand the molecular configurations of supported vanadia species are abundant in the literature. In the dehydrated state, the configurations are typically described as the distorted $VO_4$ species on the catalyst support that become, except for silica-supported materials, oligomeric as the surface density increases, comprising a mixture of species types.[10] Vanadia is well known to be strongly impacted by the chemical environment, such as the hydration state, presence of adsorbates, metal-oxide loading, and oxide-supporting material.[11] Hydration is of particular interest because of its relevance to the initial state of manufactured catalysts prior to their use and to the photocatalytic performance of vanadium-based heterogeneous catalysts[12] because water molecules are not driven from the surface under ambient conditions.[13] Under

Received: May 10, 2021
Revised: July 12, 2021
Published: July 23, 2021

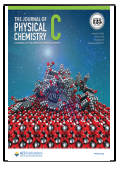







https://doi.org/10.1021/acs.jpcc.1c04150
J. Phys. Chem. C 2021, 125, 16766–16775

such hydrated conditions, vanadia is known to interact with adsorbed moisture, stimulating a structural change as a thin aqueous layer forms on the oxide support that enables vanadia to migrate and form new molecular structures.[14] To obtain a detailed molecular picture of these structures of vanadium oxide supported on titania under such conditions, nuclear magnetic resonance (NMR) was exploited as a tool to discriminate and quantify the vanadia species present on hydrated supported vanadium oxide catalytic materials.

NMR is a well-demonstrated technique that can provide specific insights into the types of molecular structures present in a sample.[15−17] As a nondestructive and quantitative spectroscopic method, it can discriminate among the chemical environments of diamagnetic nuclei by employing a strong magnetic field to manipulate the nuclear spins. Because $^{51}$ V is a quadrupolar nucleus, it is subject to quadrupolar interactions that broaden the NMR signals, decreasing spectral resolution and introducing quadrupolar line shapes. To mitigate this, high magnetic field strengths have been employed to probe the surface of supported $V_2O_5/TiO_2$ catalysts, reducing second-order contributions to the quadrupolar interactions. The $^{51}$V magic-angle spinning-nuclear magnetic resonance ($^{51}$V MAS NMR) assignments of these various vanadia species supported on titania materials have been reported on the basis of previous reports and computational modeling.[18] Furthermore, the ability to control the environment and observe the structural changes that occur under specified conditions is a notable advantage of the $^{51}$V MAS NMR spectroscopic technique.[19] We have previously discriminated the surface molecular structures of several vanadium oxide catalysts and found that SCR is promoted by the presence of oligomeric vanadia.[20] Herein, we employ similar strategies to understand the structure of these materials under hydrated conditions.

## EXPERIMENTAL METHODS

Supported vanadia and tungsta catalysts were synthesized by the incipient-wetness impregnation of the aqueous solutions of ammonium metavanadate (0.35 M, Aldrich) and/or ammonium metatungstate (0.06 M, Pfaltz & Bauer, 99.5%) onto the $TiO_2$ support (Degussa, P-25, ∼55 $m^2/g$). The resulting sample was stirred for half an hour before being dried overnight. If applicable, subsequent impregnation was repeated using the tungsta precursor to generate promoted vanadia catalysts. After all metal oxides were supported and dried, the samples were dried with flowing air (0.1 L/min) at 120 °C for 4 h and then thermally treated at 550 °C for 4 h under flowing air. Temperature ramp rates during the synthesis were controlled to 1 °C/min.

Prior to NMR measurements, dehydrated catalyst samples were dried in flowing dry air (∼20 sccm/mg) at 400 °C for 3 h. The samples were sealed inside a thermal treatment tube with isolation valves at the conclusion of the thermal treatment and subsequently transferred to a nitrogen-filled glovebox. Inside the dry box, the samples were loaded into 2.5 mm pencil-type Bruker NMR rotors for NMR analysis. Hydrated samples contacted air for several months prior to loading into the NMR rotors with no additional treatment. The temperature during storage was 23 °C in climate-controlled environments with an approximate water pressure of 1.2 kPa.

The $^{51}$V MAS NMR experiments were conducted using a 14.0921 T Bruker wide-bore spectrometer equipped with a commercial 2.5 mm pencil-type MAS probe. The corresponding 51 V Larmor frequency is 157.777832 MHz. Single-pulse $^{51}$V NMR experiments were conducted with a $\pi/6$ pulse width of 1.5 $\mu$s, a delay time of 0.2 s, a spectral width of 1 MHz, and an acquisition time of 4.096 ms. While this deviates from the generally accepted $\pi/10$ criterion for confidence in the quantitative nature of spectra of quadrupolar nuclei,[21] this approximation allows for the enhanced sensitivity required for this dilute and broad species and enables the collection of largely quantitative results. It also lies within the realm of tip angles previously employed by other research groups for such systems,[22] including a work which demonstrated that tip angles less than $\pi/3$ were sufficient for accurate representation of relative intensities.[23] It should be stated that the primary interaction for $^{51}$V NMR is chemical-shift anisotropy and that quadrupolar interactions are relatively minor contributions[24,25] and that MAS NMR is an effective way to detect small changes in the chemical shift between different vanadia species.[24,26] Because chemical-shift anisotropy is an informative and important consideration for vanadium NMR, the full array of parameters is ideally extracted using satellite transition spectroscopy (SATRAS).[27−29] An accurate analysis of the sideband pattern to extract such parameters is unfortunately stressed by complicated baselines, poor sensitivity of dilute supported oxides, and extensive probe ringdown. Typically, 389,120 scans were collected per $^{51}$V MAS NMR spectrum. Chemical shifts were externally referenced to the center band of bulk $V_2O_5$ at −613.8 ppm relative to $VOCl_3$. Spinning rates of 32−35 kHz were used for all 600 MHz experiments. To abate concerns regarding the potential presence of NMR-invisible $V^{4+}$ species, we have previously performed quantitative electron paramagnetic resonance measurements on the dehydrated samples and have reported less than 1% of all vanadium in the reduced state.[20] Reduction in the hydrated condition is neither expected nor extensively shown for other materials,[30] so the presented NMR should be regarded as representative of the vanadium species present in the catalyst.

The $^{1}$H MAS NMR experiments were conducted to ensure the dry or hydrated state of the catalyst surface before and after the $^{51}$V MAS NMR measurement, which is evidenced by the absence or presence of water in the $^{1}$H NMR signal. A representative example is provided in Figure S2. A $5\pi/24$ pulse width of 1.25 $\mu$s, a delay time of 2 s, a spectral width of 0.5 MHz, and an acquisition time of 8.192 ms comprised the pulse sequence. Typically, 1,024 scans were collected per $^{1}$H MAS NMR spectrum. The $^{1}$H chemical shifts were externally referenced to adamantine at 1.82 ppm.

The interpretation of the NMR spectra was assisted by NMR chemical-shift calculations rooted in density functional theory using the Amsterdam density functional (ADF) software.[31−33] Cluster model geometries were optimized using the generalized gradient approximation (GGA) with Grimme's third-generation dispersion corrections applied to the Beck-Lee-Yang-Parr functional (GGA: BLYP-3D).[34−36] Scalar relativistic effects were accounted for using the zero-order regular approximation (ZORA).[37,38] The slater-type, all-electron, triple- $\zeta$, two-polarization function (TZ2P) was implemented as the basis set.[39]

Anatase $TiO_2$ surface cluster models were constructed from Howard et al.'s structural determination of anatase cut along the (001) and (101) planes.[40] The models provided two layers of repeating lattice titania in depth, where the bottom layer was frozen to preserve the crystal structure, allowing the surface and the first row below to relax. Terminal oxygen atoms were charge-balanced with protons at a length of 9.7 Å in the


https://doi.org/10.1021/acs.jpcc.1c04150
J. Phys. Chem. C 2021, 125, 16766−16775

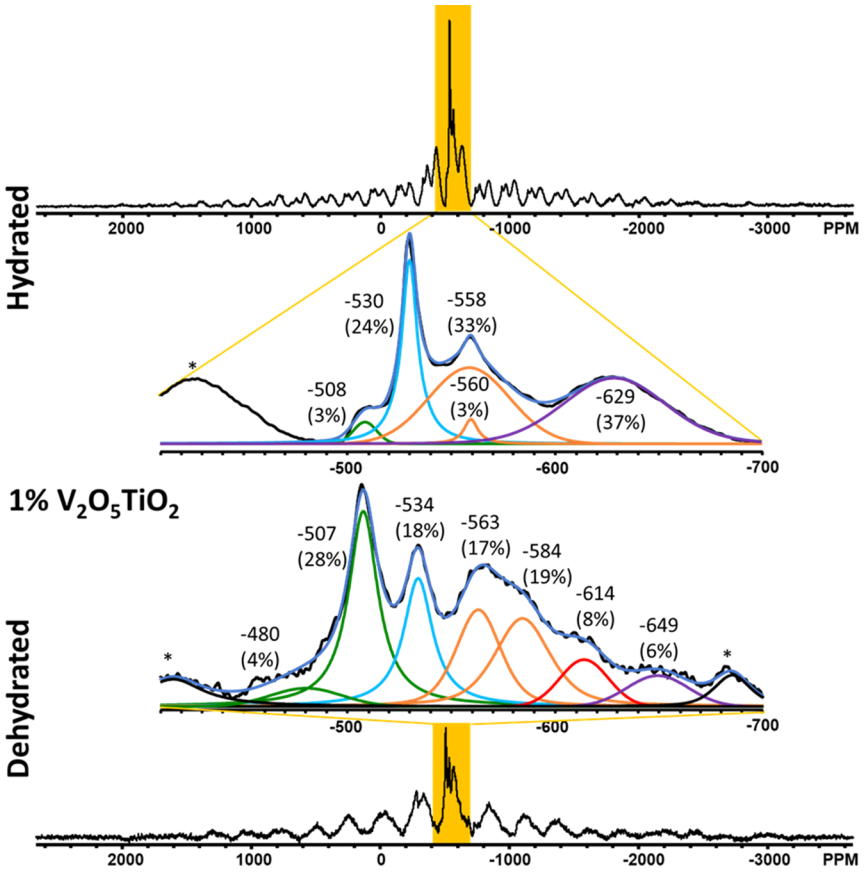


**Figure 1.** In situ $^{51}$V MAS NMR of the supported 1% $V_2O_5/TiO_2$ catalyst under hydrated (top) and dehydrated (bottom) conditions. The center band has been expanded for clarity. * indicates the spinning side band.

direction of the removed Ti atoms. Vanadium oxide species were arranged atop this surface model and optimized as described above.

Vanadium oxytrichloride ($VOCl_3$) at 0 ppm was used as the computational standard to compare the theoretical results to the experimental findings (shielding of −1858.09).[41,42] The calculated shielding relates to the chemical shift by $\delta(^{51}V) = -1858.09-\sigma_{calc}$. A secondary reference, $V_2O_5$, correlates to the experimental results of −613.8 ppm at −618 and −607 ppm for the ensemble average and center vanadium atoms, respectively, validating the method.

## RESULTS AND DISCUSSION

**Low Surface Vanadia Density of Titania-Supported Vanadia Catalysts.** When occupying a support at low surface vanadia densities, vanadium oxide is prescribed to resemble primarily monomeric vanadia species.[20] The 1% $V_2O_5/TiO_2$ material presented herein corresponds to a surface density of ∼1 V/nm$^2$, which is consistent with low coverage conditions because a monolayer of vanadia corresponds to 8 V/nm$^2$. This supported $V_2O_5/TiO_2$ catalyst, with 0.13$\theta$ of monolayer coverage, is known to show preferential formulation of monomeric species under dehydrated conditions, but still a distribution of vanadia species occupies the surface. To gain further insights into the type of vanadia species present, solid-state $^{51}$V MAS NMR was employed to discriminate the structures of vanadia in the sample. The relevant results are depicted in Figure 1.

Under dehydrated conditions, an assortment of signals is present that have been detailed previously.[20] Briefly, signals at −507 and −534 ppm correspond to $VO_4$ and square-pyramidal-type $VO_5$ monomeric species anchored to the titania surface. Broad signals downfield may be indicative of monomeric species near an oxygen vacancy; however, this is supported primarily by computational correlations shown in a previous work.[20] Furthermore, such species tentatively deconvoluted at −480 ppm are quite broad and exhibit low intensity, increasing uncertainty in the origin of such species. All isolated vanadia signals account for 50% of the integrated spectral intensity of the center band. It can be seen from the spinning side-band pattern that differences in chemical-shift anisotropy between individual chemical species may be over-representing the monomers in the center band intensity; however, for the purposes of comparison to the same sample, the center band is used. This quantification imprecision is less impactful on samples containing primarily oligomers (see below), for which side bands retain their shape.[43] The assignment for signals near −562 ppm has evolved over the years, previously being ascribed to a variety of features including $VO_4$ oligomers,[17] distorted $VO_4$,[44] and more recently affirmed as dimers ($V_2O_7$).[18] Such dimeric vanadia species at −563 and −584 ppm account for about 38% of the vanadia observed. Signals upfield at −614 and −649 ppm are ascribed to polyvanadate in oligomeric species. It should be noted that the $^{51}$V signals at −614 ppm typically correspond to bulk $V_2O_5$; however, such polycrystalline nanoparticles that form when the monolayer is exceeded are typically narrower in nature because of vanadia site uniformity and exhibit a distinct spinning side-band pattern. The absence of both characteristics leads to the assessment that these species are dehydrated


https://doi.org/10.1021/acs.jpcc.1c04150
J. Phys. Chem. C 2021, 125, 16766−16775

oligomeric surface vanadia, which may be precursors to the well-defined bulk $V_2O_5$ polycrystalline structure.

Distinct changes to the spectrum are observed when the sample contacts water vapor. The top of Figure 1 highlights the vanadia chemical environments that arise from $0.13\theta$ $V_2O_5/TiO_2$ that underwent exposure to ambient moisture over an extended period of time. Notably, signals corresponding to $VO_4$ monomers at −508 ppm are suppressed, comprising only 3% of the total signal for the hydrated sample. In contrast, the intensity at the position of the distorted $VO_5$ species is mildly enhanced under hydrated conditions, up to 24% from 18%. Changes are also observed in the intermediate chemical shift range, where the intensity near −583 ppm is suppressed in favor of both a broad and narrow resonance at −560 ppm, and both signals comprise 36% of the integrated total $^{51}V$ NMR signal intensity. Finally, a dramatic enhancement (from 14% to 37%) of signals indicative of vanadia oligomers at −630 ppm is observed, which suggests that under hydrated conditions, the vanadia species can migrate and combine to generate oligomeric vanadia species, expressing a higher abundance of such species relative to their dehydrated counterparts.

These results are slightly dissimilar to what has been previously reported for silica-supported vanadium oxide catalysts. In the case of a hydrated $V_2O_5/SiO_2$ materials, all vanadia resonances dramatically change across a range of surface densities.[10,30,45] Here, only a portion of the vanadia is transformed to more oligomeric structures. Such contrast may reflect the stronger interaction between titania and vanadium oxide relative to that for the silica support. This, in turn, renders surface vanadia species more stable on titania (the V−O-Support bonds may be less hydrolyzed in moisture).

To better discriminate the potential impact water has on the shielding of vanadia nuclei, computational modeling efforts were explored (Figure 2). Distorted $VO_4$ monomers exhibit a slight shift upfield in the presence of water, depending on the surface proton placement (Figure 2a,b). This prediction may accurately account for a portion of the signal enhancement of distorted $VO_5$ species under hydrated environments. Dimeric species with two V−O−V linkages (Figure 2c) result in chemical-shift predictions that are relatively unaffected by the presence of water (−541 ppm without water to −550 ppm when hydrated), which is similar to the chemical shift assigned to dehydrated dimeric vanadia species in the NMR spectra. The enhancement of signals in this region may be due to the migration of isolated surface vanadia species, which agglomerate to form this dimeric configuration. Attempts were also made to assess the potential for the hydrolysis of the V−O−Ti bridge to form a stable, digrafted species (Figure 2d,e), as previously reported.[46] It has been previously predicted that at low vanadia coverages, when not rigorously dehydrated, $OV(OH)O_2$ monomers would form and possess a high affinity for water.[46,47] Such species are predicted to reflect chemical shifts near −590 or −600 ppm, the experimental results of which show a loss of intensity upon hydration, suggesting the need for revised models.

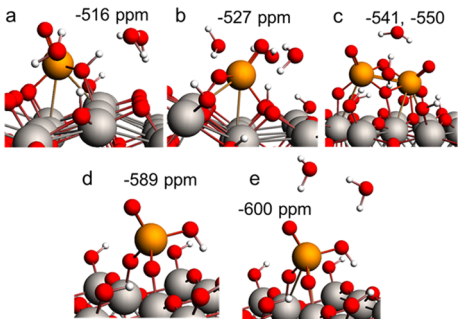


**Figure 2.** DFT-optimized cluster models of hydrated vanadium oxide structures on $TiO_2$, including (a) distorted $VO_4$ with bridge bond protonation, (b) distorted $VO_4$, (c) dibridged dimers, (d) dehydrated $VO_4$ with a hydrolyzed bridge bond, and (e) $VO_4$ with a hydrolyzed bridge bond. Atoms represented include vanadium (orange), titanium (gray), oxygen (red), and hydrogen (white).

Given the observations from the density functional theory-NMR (DFT-NMR) calculations, it can be explained that under hydrated conditions at low surface vanadia densities, a sizable portion of the vanadia species migrates on the surface to alter their electronic environment. Some distorted $VO_4$ species may remain stable and interact in the presence of water, enhancing the intensity of signals at −530 ppm. Most notably, a dramatic increase in extended oligomeric vanadia species is observed at −630 ppm. There is no evidence for the existence of stable digrafted monomeric species. These combined results clearly illustrate the changes in the structural configurations that vanadia species take when exposed to moisture.

**Tungsten-Promoted Titania-Supported Vanadia Catalysts.** Sometimes, tungsten oxide is incorporated as a promoter to vanadia-based catalysts on titania supports, especially for SCR applications. One of the noted benefits of tungsten oxide-promoted vanadia materials is its ability to stabilize surface vanadia species under SCR reaction conditions.[48] Indications of the extent of hydrothermal stability may be apparent even at low temperatures in the presence of water. It has also been shown that surface occupation of tungsten oxide leads to the promotion of surface vanadia species that are more oligomeric in nature.[20] To probe this, a submonolayer vanadia ($1\ V/nm^2$; $0.13\theta$) catalyst with tungsten promotion ($2.4\ W/nm^2$; $0.53\theta$), represented by the notation 1% $V_2O_5$−5% $WO_3/TiO_2$, was prepared and analyzed with $^{51}V$ MAS NMR under ambient conditions to compare with the known vanadia speciation of the dehydrated counterpart. The resulting spectra are presented in Figure 3.

As known, the presence of surface tungsta species generates large quantities of oligomeric vanadia species, even at a low vanadia coverage, under dehydrated conditions. The spectrum from the dehydrated 1% $V_2O_5$−5% $WO_3/TiO_2$ catalyst shown in Figure 3 shows small amounts of monomeric species at −517 and −535 ppm (18%) and dimeric vanadia species at −568 ppm (24%), with an abundance of oligomeric vanadia species at −630 ppm (58%). When hydrated, the changes to the structure of vanadia species are notable, but not as significant as with the tungsta-free vanadia catalyst. Under hydrated conditions, the monomeric vanadia species are suppressed to the point of not being clearly resolved from the dimeric vanadia species at −553 ppm. The types of oligomeric vanadia species appear to change slightly, which is evidenced by a relatively narrow resonance at −623 ppm and a shoulder at −660 ppm. These are in the region typically ascribed to oligomers, but the oligomer abundance is comparable to that of the corresponding dehydrated catalyst.

Because of the relatively narrow nature and the chemical shift position of the feature at −623 ppm, it may follow that this peak could be related to the further migration of vanadia species to form bulk $V_2O_5$ crystallites. To assess this possibility, the spinning side-band pattern of the hydrated spectrum's


https://doi.org/10.1021/acs.jpcc.1c04150
J. Phys. Chem. C 2021, 125, 16766−16775

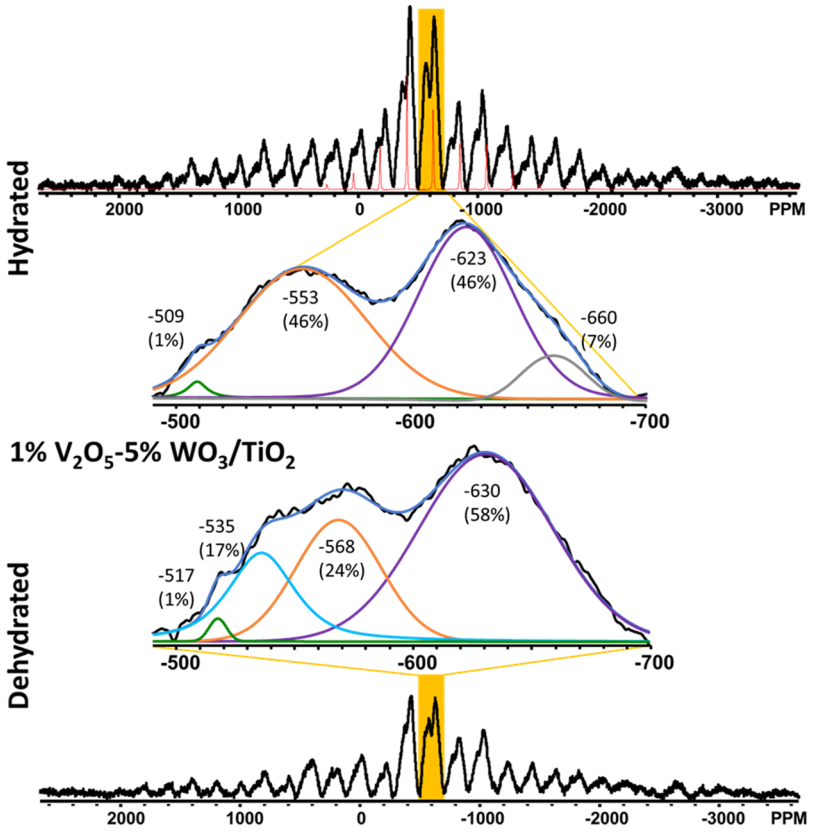


**Figure 3.** In situ $^{51}$V MAS NMR of 1% $V_2O_5$−$WO_3/TiO_2$ under hydrated (top) and dehydrated (bottom) conditions. The center band has been expanded for clarity. The spectrum for bulk $V_2O_5$ (red) has been overlaid for comparison.

−623 ppm peak was compared to that of bulk $V_2O_5$ (red overlay, at a slightly faster spinning rate). It is apparent that the spinning side-band pattern of the bulk material dissipates much faster than the peak at −623 ppm, indicating that these two features are dissimilar, with the catalyst signal having larger quadrupolar coupling than the well-defined crystal. Indeed, larger quadrupolar coupling is expected of vanadia strongly bound to a support surface.[49,50] Given that the species present under hydrated conditions are quite similar to those under dry conditions, it follows that tungsten oxide indeed assists to stabilize the surface vanadia species as oligomers. Even the initially present oligomers resist agglomeration to generate $V_2O_5$ crystallites in the presence of the tungsta promoter. Such an observation has implications on the previously reported effects of these materials when (hydro)thermally aged. Marberger et al. noted some vanadia species were more volatile than others, with potential losses in vanadium up to 0.8% under the reported conditions of hydrothermal aging.[51] Increased SCR activity upon exposing the catalysts to increasingly harsh thermal treatments was noted and attributed to decreases in the surface area overcoming losses to catalytically active vanadium atoms. This may well be due to the redistribution of surface vanadia to occupy more oligomeric configurations that are relatively resistant to hydrothermal treatment in a fashion similar to the oligomerization observed in the presence of tungsten and the concomitant increase in vanadium stability afforded by the presence of tungsten oxide. Indeed, the extent of oligomerization tends to increase with surface tungsten oxide coverage as well as calcination temperature.[52] Hydrothermal aging trends suggest similar responses, but with some variability at very high tungsten concentrations. Such thermal aging practices may work cooperatively with tungsten oxide to enhance $V_2O_5$−$WO_3/TiO_2$ SCR catalysts.

**High Surface Density Titania-Supported Vanadia Catalysts.** The effect of moisture on near-monolayer surface vanadia catalysts was also considered to better understand the origin of the hydration stability for 1% $V_2O_5$−5% $WO_3/TiO_2$. The presence of tungsten oxide alone could offer such an effect, but it is also possible that such a property is inherent to the nature of vanadia oligomers. A supported 5% $V_2O_5/TiO_2$ catalyst (7 V/nm$^2$; 0.88$\theta$) was analyzed under hydrated and dehydrated conditions with $^{51}$V MAS NMR, and the resulting spectra are presented in Figure 4. The dehydrated catalyst exhibits an array of surface vanadia signatures that correspond to monomers (−526 and −544 ppm; 7%), dimers (−580 ppm; 54%), bulk-like $V_2O_5$ (−612 ppm; 13%), and oligomeric vanadia (−645 ppm; 26%) surface species. Previously, it was uncertain whether the −612 ppm feature in this sample was related to bulk $V_2O_5$; however, the comparison of the spinning side-band pattern of the dehydrated catalyst to that of bulk $V_2O_5$ indicates that these species are likely polycrystalline $V_2O_5$ nanoparticles within the limits of the local structure sensitivity of NMR, but polycrystalline $V_2O_5$ was not present in the Raman spectrum of this dehydrated catalyst.

Upon hydration, a dramatic change is observed in the $^{51}$V NMR spectrum for the 5% $V_2O_5/TiO_2$ catalyst. Under such conditions, the catalyst exhibits a narrow distribution of vanadia with only two distinct, relatively narrow environments. The primary feature resonates at −614 ppm, exhibits a spinning side-band pattern consistent with bulk $V_2O_5$, and represents 95% of all vanadia in the catalyst. Under the



https://doi.org/10.1021/acs.jpcc.1c04150
J. Phys. Chem. C 2021, 125, 16766−16775

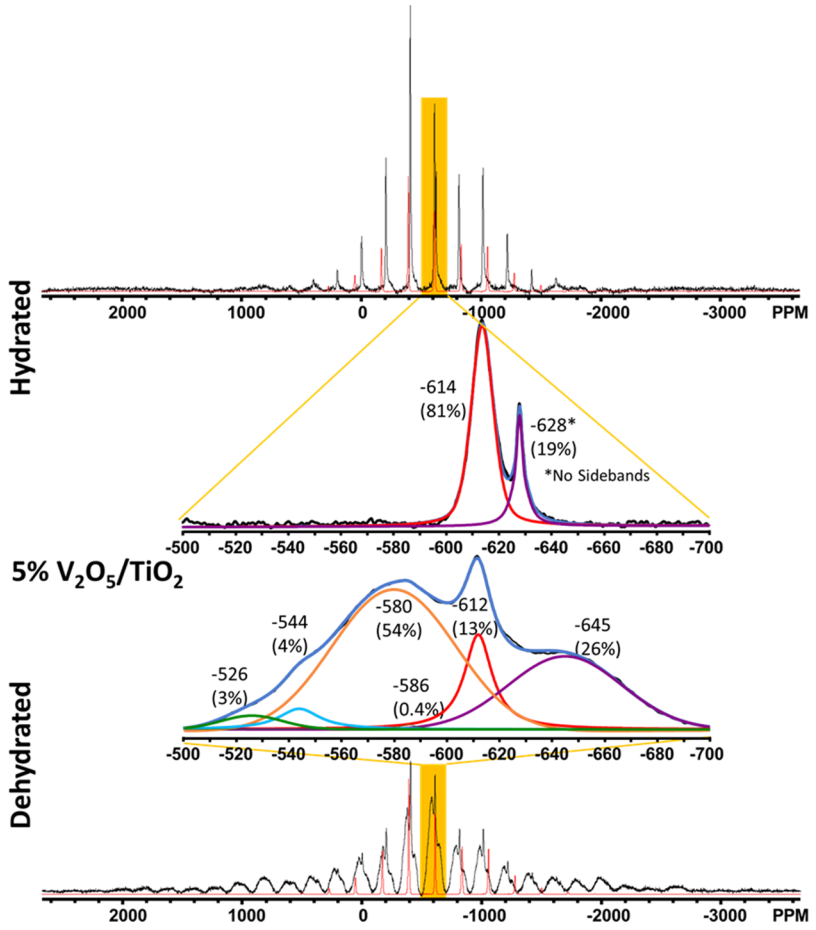


**Figure 4.** In situ $^{51}$V MAS NMR of 5% $V_2O_5/TiO_2$ under hydrated (top) and dehydrated (bottom) conditions. The center band has been expanded for clarity. The spectrum for bulk $V_2O_5$ (red) has been overlaid for comparison.

conditions of hydration at high surface vanadia densities, migration and agglomeration of vanadia species to generate these bulk $V_2O_5$ nanoparticles are apparent. Interestingly, a second, very narrow resonance is present at −628 ppm, accounting for just 5% of the environments. This species produces no obvious spinning side-band pattern, reflecting a vanadia species that is relatively mobile. Indeed, it has been predicted that high levels of hydration can stimulate the leaching of $OV(OH)_3$ species.[46] Although previously proposed,[53] this study represents the first time that a fraction of vanadia species was distinctly observed as a dissolved vanadia species on the titania surface under hydrated conditions.

To better understand the type of mobile vanadia species present on a wetted surface, a vanadia solution phase diagram can be employed to describe the dissolved vanadia species.[54] This phase diagram, reconstructed and adopted in Figure S3, describes the configurations that vanadia species take under varying pH and concentrations. The pH of an overlayer solution on a hydrated metal-oxide surface can be approximated by the average between the point of zero charge (PZC) of the support and of the anchored metal-oxide phase. In the case of vanadia (PZC: 1.5) on titania (PZC: 6.2), the pH acting on these species should be approximately 3.9. Note that in the presence of tungsten oxide (PZC: 1.5), the pH can be approximated at 3.1. According to the phase diagram, vanadia in solution on the titania surface should occupy either decavanadate ($V_{10}O_{26}(OH)_2^{2-}$) or $VO(OH)_3$ structures at such conditions, depending on the concentration of vanadia in solution. Decavandate, favored at high concentrations, should exhibit multiple chemical-shift signatures and may be too bulky for fast molecular tumbling when confined to a layer of water on the surface of titania (note that it can do so in aqueous solutions), so this species is discounted.[30,55] As such, the mobile vanadia species at −628 ppm is tentatively assigned to $VO(OH)_3$. We previously modeled a cluster of $VO(OH)_3$ in vacuum to yield a predicted chemical shift of −574 ppm.[35] Attempts were made to model potential configurations in explicit water as the solvent while proximal to the surface of titania, including a monografted $VO_X$ species, but the calculated shielding results suggest chemical shifts between −430 and −480 ppm instead (Figure S1), which are inconsistent with the experimental observations.

The $^{51}$V NMR chemical shifts of various vanadate solutions across different concentrations and pH levels have been reported previously. A number of metavanadate ions in aqueous solutions across a range of pH values show poor agreement with the observed mobile phase feature reported herein (and summarized in Figure S3).[56−61] Likewise, the chemical shift of $VO(O_2)^{2-}$ has been explored over a range of pH values and counterions, but it does not reflect the species from our $^{51}$V MAS NMR spectrum.[62] Interestingly, Conte et al. explored combinations of $NH_4VO_2$, $H_2O_2$, and picolinic acid in water at different pH values. They observed a vanadia species near this chemical shift: $VO(O_2)PIC_2^-$, a monoperoxo vanadium complex with two picolinate ligands. Given the lack of picolinic acid, this is unlikely the identity of the dissolved


https://doi.org/10.1021/acs.jpcc.1c04150
J. Phys. Chem. C 2021, 125, 16766−16775

surface species. It is also interesting to note that solutions of oxovanadium trimethoxide, oxovanadium triethoxide, and oxovanadium triisopropoxide have been reported at −600, −590, and −630 ppm, respectively.[55] The consistency between these reported values and the experimental value reported here leads to the assignment of a mobile vanadia species in the solution that exhibits a chemical environment similar to that of oxovanadium alkoxide species, such as $O{=}V(OCH_2CH_3)_3$, on the basis of the chemical shift, but different in the absolute coordination environment, given our lack of alkoxides in the system. Organic species contributing to 5% of the vanadium signal must either come from the oxalic acid synthesis procedure, the titania support, or form from trace organic vapors found in air and survive thermal treatment in air at 550 °C. Given that these samples were previously shown to be free to impurities, organic species would decompose at elevated temperatures, no alkoxide or alcohols were used in the system, and any present would promptly hydrolyze in the presence of water (ambient spectra), it is unlikely that such species explain the observation of the mobile peak in this work. Furthermore, a systematic study of the effect of titania impurities on the $^{51}V$ NMR spectra did not show such a species, suggesting that this signal does not arise from the presence of one of the tested impurities.[23] Potentially, $O{=}V(OH)_3$ species are distorted by the titania surface functional groups that alter the observed chemical environment from what would be expected from the solution state of $VO(OH)_3$; however, a consistent theoretical model was not found. Our DFT models predict that the chemical shift of $VO(OH)_3$ species does not change appreciably with water exposure. Given the preponderance of evidence, this species is broadly described by a mobile vanadium species that is solvated using water.

When the dry high-density surface vanadia species are exposed to moisture, the anchored vanadium oxide species can hydrolyze their support bonds and migrate to form larger oligomeric clusters. At a high enough surface vanadia density, the primary structure generated is that of bulk polycrystalline $V_2O_5$. Residual hydrolyzed vanadium species remain detached from the support surface and are mobile in solutions. They occupy molecular configurations that express chemical environments similar to those of oxovanadium alkoxide species and are tentatively assigned as the $VO_x$ species that are mobile yet maintain interactions with surface titania sites that may keep them localized or in environments dissimilar to a truly aqueous $VO(OH)_3$ species. Such a result not only highlights the dramatic structural changes that take place in the presence of water but also supports previous findings[63,64] that additives such as tungsten oxide stabilizes the vanadia species because the oligomeric vanadia species present in the promoted catalyst do not aggregate to form $V_2O_5$ nanoparticles, whereas those oligomeric species in the unpromoted vanadia catalyst do form $V_2O_5$ nanoparticles. This observation accounts for the relatively common observation of $V_2O_5$ or other metal-oxide crystallites in hydrated catalysts and the absence of the crystallites in dehydrated catalysts as probed by Raman spectroscopy.

The generality of using the metal-oxide phase diagram to predict the vanadium speciation of a wet metal oxide surface is not supported by the current experimental results. Indeed, several studies have examined the $^{51}V$ NMR spectra of vanadia species in solutions at different pH, concentrations, and counter-anion conditions. Figure S3 presents the chemical shifts observed for various vanadia species in solutions in the context of such a phase diagram. The poor agreement with our own experimental results suggests that the support plays a role in directing the chemical environment of the vanadium oxide atoms beyond altering the isoelectric point (PZC). While the immediate bonding environment of vanadia may be directed by such a phase diagram [such as $VO(OH)_3$], the specific geometry of such molecular configurations is impacted by the oxide support, which may express functionalities that perturb the species-bonding environment of the wet vanadia moiety when compared to aqueous vanadia. This result may have implications on the molecular configurations that mobile vanadia species take when present on the surface of other hydrated supports.

## CONCLUSIONS

The present investigation describes the impact of hydration under ambient conditions on the molecular structures of titania-supported vanadium oxide catalytic materials, as monitored by magnetic resonance spectroscopy. Under hydrated conditions, surface vanadia species undergo rearrangement of their molecular structures to favor more oligomerized species compared to the dehydrated surface. At low surface vanadia densities, moderate changes to the vanadia structures are observed that slightly favor the formation of oligomerized surface vanadia species relative to the dehydrated surface. The presence of tungsten oxide as a promoter results in more stable oligomeric surface vanadia species that are not significantly impacted by hydration. This effect stems directly from the presence of surface tungsta species and not potential stabilization induced by the oligomerized vanadia species, which is evidenced by a catalyst containing high surface vanadia density that also preferentially forms oligomerized species when dehydrated but changes dramatically upon hydration. The high surface vanadia density catalyst transforms the dehydrated surface vanadia species to bulk $V_2O_5$ polycrystalline nanoparticles upon hydration, as well as the mobile vanadia species solvated by water on the titania surface. This is the first time that a fraction of anchored surface vanadia species could be discriminated from dissolved vanadia species on a wet supported vanadia catalyst. The results illustrate the strong effect that environment has on the molecular structures of metal-oxide catalysts. The current observations for vanadium oxide have broad implications for how the structures of other metal-oxide materials are altered upon hydration, laying the framework for a molecular-level understanding of the structures of hydrated metal-oxide catalysts.

## ASSOCIATED CONTENT

### Supporting Information

The Supporting Information is available free of charge at https://pubs.acs.org/doi/10.1021/acs.jpcc.1c04150.

DFT-optimized geometry depictions and coordinates (PDF)

## AUTHOR INFORMATION

### Corresponding Authors

**Yong Wang** − *Institute for Integrated Catalysis, Pacific Northwest National Laboratory, Richland, Washington 99354, United States; Voiland School of Chemical Engineering and Bioengineering, Washington State University, Pullman, Washington 99163, United States;* orcid.org/



https://doi.org/10.1021/acs.jpcc.1c04150
J. Phys. Chem. C 2021, 125, 16766−16775

0000-0002-8460-7410; Phone: 509-371-6273; Email: yong.wang@pnnl.gov

**Jian Zhi Hu** − *Institute for Integrated Catalysis, Pacific Northwest National Laboratory, Richland, Washington 99354, United States; Voiland School of Chemical Engineering and Bioengineering, Washington State University, Pullman, Washington 99163, United States;* orcid.org/0000-0001-8879-747X; Phone: 509-371-6544; Email: jianzhi.hu@pnnl.gov

**Israel E. Wachs** − *Operando Molecular Spectroscopy & Catalysis Laboratory, Department of Chemical & Biomolecular Engineering, Lehigh University, Bethlehem, Pennsylvania 18015, United States;* orcid.org/0000-0001-5282-128X; Phone: 610-758-4274; Email: iew0@lehigh.edu

### Author

**Nicholas R. Jaegers** − *Institute for Integrated Catalysis, Pacific Northwest National Laboratory, Richland, Washington 99354, United States; Voiland School of Chemical Engineering and Bioengineering, Washington State University, Pullman, Washington 99163, United States;* orcid.org/0000-0002-9930-7672

Complete contact information is available at: https://pubs.acs.org/10.1021/acs.jpcc.1c04150

### Notes

The authors declare no competing financial interest.

## ■ ACKNOWLEDGMENTS

The research at Pacific Northwest National Laboratory (PNNL) was supported by the U.S. Department of Energy (DOE), Office of Science, Office of Basic Energy Sciences, Division of Chemical Sciences, Geosciences, and Biosciences. The research at Lehigh University was supported by the Center for Understanding and Control of Acid Gas-Induced Evolution of Materials for Energy (UNCAGE-ME), an Energy Frontier Research Center funded by DOE, Office of Science, Office of Basic Energy Sciences, under grant DE-SC0012577. Experiments were conducted in the Environmental Molecular Sciences Laboratory (EMSL) (grid.436923.9), a DOE Office of Science User Facility sponsored by the Office of Biological and Environmental Research and located at PNNL. NMR experiments were conducted in part using a Bruker 600 MHz NMR spectrometer acquired with the support from the U.S. Department of Energy, Office of Science, Office of Basic Energy Sciences (Project Number 66628). EMSL's supercomputers were utilized as a resource for computational modeling. PNNL is a multiprogram national laboratory operated by Battelle for the U.S. Department of Energy under Contract DE-AC05-76RL01830.

## ■ REFERENCES

(1) Rostom, S.; de Lasa, H. Propane Oxidative Dehydrogenation on Vanadium-Based Catalysts under Oxygen-Free Atmospheres. *Catalysts* **2020**, *10*, 418.

(2) Cozzolino, M.; Tesser, R.; Diserio, M.; Donofrio, P.; Santacesaria, E. Kinetics of the Oxidative Dehydrogenation (Odh) of Methanol to Formaldehyde by Supported Vanadium-Based Nanocatalysts. *Catal. Today* **2007**, *128*, 191−200.

(3) Colom, J. M.; Alzueta, M. U.; Christensen, J. M.; Glarborg, P.; Cordtz, R.; Schramm, J. Importance of Vanadium-Catalyzed Oxidation of So2 to So3 in Two Stroke Marine Diesel Engines. *Energy Fuels* **2016**, *30*, 6098−6102.

(4) Eversfield, P.; Lange, T.; Hunger, M.; Klemm, E. Selective Oxidation of O-Xylene to Phthalic Anhydride on Tungsten, Tin, and Potassium Promoted Vox on Tio2 Monolayer Catalysts. *Catal. Today* **2019**, *333*, 120−126.

(5) Topsoe, N. Y.; Dumesic, J. A.; Topsoe, H. Vanadia-Titania Catalysts for Selective Catalytic Reduction of Nitric-Oxide by Ammonia: I.I. Studies of Active Sites and Formulation of Catalytic Cycles. *J. Catal.* **1995**, *151*, 241−252.

(6) Shen, T. F. R.; Lai, M. H.; Yang, T. C. K.; Fu, I. P.; Liang, N. Y.; Chen, W. T. Photocatalytic Production of Hydrogen by Vanadium Oxides under Visible Light Irradiation. *J. Taiwan Inst. Chem. Eng.* **2012**, *43*, 95−101.

(7) Wachs, I. E. Recent Conceptual Advances in the Catalysis Science of Mixed Metal Oxide Catalytic Materials. *Catal. Today* **2005**, *100*, 79−94.

(8) Wachs, I. E. Catalysis Science of Supported Vanadium Oxide Catalysts. *Dalton Trans.* **2013**, *42*, 11762−11769.

(9) Guerrero-Pérez, M. O. Supported, Bulk and Bulk-Supported Vanadium Oxide Catalysts: A Short Review with an Historical Perspective. *Catal. Today* **2017**, *285*, 226−233.

(10) Das, N.; Eckert, H.; Hu, H.; Wachs, I. E.; Walzer, J. F.; Feher, F. J. Bonding States of Surface Vanadium(V) Oxide Phases on Silica: Structural Characterization by Vanadium-51 NMR and Raman Spectroscopy. *J. Phys. Chem.* **1993**, *97*, 8240−8243.

(11) Deo, G.; Turek, A. M.; Wachs, I. E.; Machej, T.; Haber, J.; Das, N.; Eckert, H.; Hirt, A. M. Physical and Chemical Characterization of Surface Vanadium-Oxide Supported on Titania - Influence of the Titania Phase (Anatase, Rutile, Brookite and B). *Appl. Catal. A-Gen.* **1992**, *91*, 27−42.

(12) Kortewille, B.; Wachs, I. E.; Cibura, N.; Pfingsten, O.; Bacher, G.; Muhler, M.; Strunk, J. Proof of Equivalent Catalytic Functionality Upon Photon-Induced and Thermal Activation of Supported Isolated Vanadia Species in Methanol Oxidation. *ChemCatChem* **2018**, *10*, 2360−2364.

(13) Jehng, J. M.; Deo, G.; Weckhuysen, B. M.; Wachs, I. E. Effect of Water Vapor on the Molecular Structures of Supported Vanadium Oxide Catalysts at Elevated Temperatures. *J. Mol. Catal. A-Chem.* **1996**, *110*, 41−54.

(14) Kortewille, B.; Wachs, I. E.; Cibura, N.; Pfingsten, O.; Bacher, G.; Muhler, M.; Strunk, J. Photocatalytic Methanol Oxidation by Supported Vanadium Oxide Species: Influence of Support and Degree of Oligomerization. *Eur. J. Inorg. Chem.* **2018**, 3725−3735.

(15) Jaegers, N. R. *Applications of in Situ Magnetic Resonance Spectroscopy for Structural Analysis of Oxide-Supported Catalysts*. Washington State University, 2019.

(16) Eckert, H.; Wacjs, I. E. 51v Nmr: A New Probe of Structure and Bonding in Catalysts. *MRS Proc.* **1987**, *111*, 459.

(17) Eckert, H.; Wachs, I. E. Solid-State Vanadium-51 Nmr Structural Studies on Supported Vanadium(V) Oxide Catalysts: Vanadium Oxide Surface Layers on Alumina and Titania Supports. *J. Phys. Chem.* **1989**, *93*, 6796.

(18) Hu, J. Z.; Hu, M. Y.; Zhao, Z. C.; Xu, S. C.; Vjunov, A.; Shi, H.; Camaioni, D. M.; Peden, C. H. F.; Lercher, J. A. Sealed Rotors for in Situ High Temperature High Pressure Mas Nmr. *Chem. Commun.* **2015**, *51*, 13458−13461.

(19) Jaegers, N. R.; Mueller, K. T.; Wang, Y.; Hu, J. Z. Variable Temperature and Pressure Operando Mas Nmr for Catalysis Science and Related Materials. *Acc. Chem. Res.* **2020**, *53*, 611−619.

(20) Jaegers, N. R.; Lai, J. K.; He, Y.; Walter, E.; Dixon, D. A.; Vasiliu, M.; Chen, Y.; Wang, C.; Hu, M. Y.; Mueller, K. T.; Wachs, I. E.; Wang, Y.; Hu, J. Z. Mechanism by Which Tungsten Oxide Promotes the Activity of Supported V2o5/Tio2 Catalysts for NOx Abatement: Structural Effects Revealed by V-51 Mas Nmr Spectroscopy. *Angew. Chem., Int. Ed.* **2019**, *58*, 12609−12616.

(21) Nielsen, N. C.; Bildsøe, H.; Jakobsen, H. J. Finite Rf Pulse Excitation in Mas Nmr of Quadrupolar Nuclei - Quantitative Aspects and Multiple-Quantum Excitation. *Chem. Phys. Lett.* **1992**, *191*, 205−212.

(22) Gheorghe, C.; Gee, B. Solid-State Vanadium-51 Nmr Studies of Supported V2o5-Wo3/Tio2 Catalysts. *Chem. Mater.* **2000**, *12*, 682−685.
(23) Eckert, H.; Deo, G.; Wachs, I. E.; Hirt, A. M. Solid-State V-51 Nmr Structural Studies of Vanadium(V) Oxide Catalysts Supported on Tio2(Anatase) and Tio2(Rutile) - the Influence of Surface Impurities on the Vanadium(V) Coordination. *Colloids Surf.* **1990**, *45*, 347−359.
(24) Lapina, O. B.; Terskikh, V. V. Quadrupolar Metal Nmr of Oxide Materials Including Catalysts. *eMagRes* **2011**, 1−21.
(25) Lapina, O. B.; Mastikhin, V. M.; Shubin, A. A.; Krasilnikov, V. N.; Zamaraev, K. I. V-51 Solid-State Nmr-Studies of Vanadia Based Catalysts. *Prog. Nucl. Magn. Reson. Spectrosc.* **1992**, *24*, 457−525.
(26) Femandez, C.; Guelton, M. Chapter 5.1 Characterization of V2o5/Tio2 Catalysts by Solid State Nmr of 51v. *Catal. Today* **1994**, *20*, 77−86.
(27) Skibsted, J.; Nielsen, N. C.; Bildsøe, H.; Jakobsen, H. J. V-51 Mas Nmr-Spectroscopy - Determination of Quadrupole and Anisotropic Shielding Tensors, Including the Relative Orientation of Their Principal-Axis Systems. *Chem. Phys. Lett.* **1992**, *188*, 405−412.
(28) Skibsted, J.; Nielsen, N. C.; Bildsøe, H.; Jakobsen, H. J. Satellite Transitions in Mas Nmr-Spectra of Quadrupolar Nuclei. *J. Magn. Reson.* **1991**, *95*, 88−117.
(29) Lapina, O. B.; Khabibulin, D. F.; Shubin, A. A.; Terskikh, V. V. Practical Aspects of V-51 and Nb-93 Solid-State Nmr Spectroscopy and Applications to Oxide Materials. *Prog. Nucl. Magn. Reson. Spectrosc.* **2008**, *53*, 128−191.
(30) Jaegers, N. R.; Wan, C.; Hu, M. Y.; Vasiliu, M.; Dixon, D. A.; Walter, E.; Wachs, I. E.; Wang, Y.; Hu, J. Z. Investigation of Silica-Supported Vanadium Oxide Catalysts by High Field V-51 Magic-Angle Spinning Nmr. *J. Phys. Chem. C* **2017**, *121*, 6246−6254.
(31) te Velde, G.; Bickelhaupt, F. M.; Baerends, E. J.; Fonseca Guerra, C.; van Gisbergen, S. J. A.; Snijders, J. G.; Ziegler, T. Chemistry with Adf. *J. Comput. Chem.* **2001**, *22*, 931−967.
(32) Fonseca Guerra, C.; Snijders, J. G.; te Velde, G.; Baerends, E. J. Towards an Order-N DFT Method. *Theor. Chem. Acc.* **1998**, *99*, 391−403.
(33) *ADF2016 Scm, Accessed July 12, 2021* Vrije Universiteit, Amsterdam, The Netherlands, http://www.scm.com, Accessed July 12, 2021.
(34) Lee, C.; Yang, W.; Parr, R. G. Development of the Colle-Salvetti Correlation-Energy Formula into a Functional of the Electron Density. *Phys. Rev. B* **1988**, *37*, 785−789.
(35) Becke, A. D. Density-Functional Exchange-Energy Approximation with Correct Asymptotic Behavior. *Phys. Rev. A* **1988**, *38*, 3098−3100.
(36) Grimme, S.; Antony, J.; Ehrlich, S.; Krieg, H. A Consistent and Accurate Ab Initio Parametrization of Density Functional Dispersion Correction (DFT-D) for the 94 Elements H-Pu. *J. Chem. Phys.* **2010**, *132*, 154104.
(37) Lenthe, E. v.; Baerends, E. J.; Snijders, J. G. Relativistic Regular Two-Component Hamiltonians. *J. Chem. Phys.* **1993**, *99*, 4597−4610.
(38) Autschbach, J.; Ziegler, T., In *Calculation of Nmr and Epr Parameters: Teory and Applications*. Wiley-VCH & Co.: 2004; 249−264.
(39) Van Lenthe, E.; Baerends, E. J. Optimized Slater-Type Basis Sets for the Elements 1−118. *J. Comput. Chem.* **2003**, *24*, 1142−1156.
(40) Howard, C. J.; Sabine, T. M.; Dickson, F. Structural and Thermal Parameters for Rutile and Anatase. *Acta Crystallogr. Sect. B* **1991**, *47*, 462−468.
(41) Justino, L. L. G.; Ramos, M. L.; Kaupp, M.; Burrows, H. D.; Fiolhais, C.; Gil, V. M. S. Density Functional Theory Study of the Oxoperoxo Vanadium(V) Complexes of Glycolic Acid. Structural Correlations with Nmr Chemical Shifts. *Dalton Trans.* **2009**, 9735−9745.
(42) Bjornsson, R.; Früchtl, H.; Bühl, M. 51v Nmr Parameters of Vocl3: Static and Dynamic Density Functional Study from the Gas Phase to the Bulk. *Phys. Chem. Chem. Phys.* **2011**, *13*, 619−627.
(43) Nielsen, U. G.; Topsøe, N. Y.; Brorson, M.; Skibsted, J.; Jakobsen, H. J. The Complete V-51 Mas Nmr Spectrum of Surface Vanadia Nanoparticles on Anatase (Tio2): Vanadia Surface Structure of a Deno(X) Catalyst. *J. Am. Chem. Soc.* **2004**, *126*, 4926−4933.
(44) Borovkov, V. Y.; Mikheeva, E. P.; Zhidomirov, G. M.; Lapina, O. B. Theoretical and Experimental Studies of the Nature of the Catalytic Activity of Vox/Tio2 Systems. *Kinet. Catal.* **2003**, *44*, 710−717.
(45) Schimmoeller, B.; Jiang, Y.; Pratsinis, S. E.; Baiker, A. Structure of Flame-Made Vanadia/Silica and Catalytic Behavior in the Oxidative Dehydrogenation of Propane. *J. Catal.* **2010**, *274*, 64−75.
(46) Lewandowska, A. E.; Calatayud, M.; Tielens, F.; Bañares, M. A. Dynamics of Hydration in Vanadia-Titania Catalysts at Low Loading: A Theoretical and Experimental Study. *J. Phys. Chem. C* **2011**, *115*, 24133−24142.
(47) Lewandowska, A. E.; Calatayud, M.; Tielens, F.; Bañares, M. A. Hydration Dynamics for Vanadia/Titania Catalysts at High Loading: A Combined Theoretical and Experimental Study. *J. Phys. Chem. C* **2013**, *117*, 25535−25544.
(48) Chapman, D. M. Behavior of Titania-Supported Vanadia and Tungsta SCR Catalysts at High Temperatures in Reactant Streams: Tungsten and Vanadium Oxide and Hydroxide Vapor Pressure Reduction by Surficial Stabilization. *Appl. Catal. A: Gen.* **2011**, *392*, 143−150.
(49) Lapina, O. B.; Khabibulin, D. F.; Shubin, A. A.; Bondareva, V. M. V-51 and P-31 Nmr Studies of Vox/Tio2 Catalysts Modified by Phosphorous. *J. Mol. Catal. A: Chem.* **2000**, *162*, 381−390.
(50) Shubin, A. A.; Lapina, O. B.; Bondareva, V. M. Characterisation of Strongly Bonded V(V) Species in Vox/Tio2 Catalyst by Static and Mas Solid-State V-51 Nmr Spectroscopy. *Chem. Phys. Lett.* **1999**, *302*, 341−346.
(51) Marberger, A.; Elsener, M.; Nuguid, R. J. G.; Ferri, D.; Kröcher, O. Thermal Activation and Aging of a V2o3/Wo3-Tio2 Catalyst for the Selective Catalytic Reduction of No with Nh3. *Appl. Catal. A: Gen.* **2019**, *573*, 64−72.
(52) Lai, J.-K.; Jaegers, N. R.; Mosevitzky Lis, B.; Ford, M. E.; Walter, E.; Wang, Y.; Hu, J. Z.; Wachs, I. E. Structure-Activity Relationships of Hydrothermally Aged Titania-Supported Vanadium-Tungsten Oxide Catalysts for Scr of Nox Emissions with $Nh_3$. 2021 Under Review.
(53) Lapina, O. B.; Shubin, A. A.; Nosov, A. V.; Bosch, E.; Spengler, J.; Knözinger, H. Characterization of V2o5-Tio2 Catalysts Prepared by Milling by ESR and Solid State H-1 and V-51 Nmr. *J. Phys. Chem. B* **1999**, *103*, 7599−7606.
(54) Baes, C. F.; Messmer, R. E., *The Hydrolysis of Cations*; John Wiley & Sons Inc, 1976.
(55) Lee, K. T.; Pozarnsky, G.; Zarembowitch, O.; McCormick, A. V-51 Nmr of Homogeneous Multicomponent Vanadium Oxide Solutions. *Chem. Eng. J.* **1996**, *64*, 215−223.
(56) Habayeb, M. A.; Hileman, O. E., Jr. 51v Ft-Nmr Investigations of Metavanadate Ions in Aqueous Solutions. *Can. J. Chem.* **1980**, *58*, 2255−2261.
(57) Ralston, K. D.; Chrisanti, S.; Young, T. L.; Buchheit, R. G. Corrosion Inhibition of Aluminum Alloy 2024-T3 by Aqueous Vanadium Species. *J. Electrochem. Soc.* **2008**, *155*, C350−C359.
(58) Tracey, A. S.; Jaswal, J. S.; Angus-Dunne, S. J. Influences of Ph and Ionic-Strength on Aqueous Vanadate Equilibria. *Inorg. Chem.* **1995**, *34*, 5680−5685.
(59) Howarth, O. W.; Richards, R. E. Nuclear Magnetic Resonance Study of Polyvanadate Equilibria by Use of Vanadium-51. *J. Chem. Soc.* **1965**, 864.
(60) Hatton, J. V.; Saito, Y.; Schneider, W. G. Nuclear Magnetic Resonance Investigations of Some Group V Metal Fluorides and Oxyions. *Can. J. Chem.* **1965**, *43*, 47.
(61) O'Donnell, S. E.; Pope, M. T. Applications of V-51 and P-31 Nuclear Magnetic-Resonance Spectroscopy to Study of Iso-Poly-vanadates and Hetero-Polyvanadates. *J. Chem. Soc., Dalton Trans.* **1976**, 2290−2297.


https://doi.org/10.1021/acs.jpcc.1c04150
J. Phys. Chem. C 2021, 125, 16766−16775

(62) Conte, V.; di Furia, F.; Moro, S. V-51-Nmr Investigation on the Formation of Peroxo Vanadium Complexes in Aqueous-Solution - Some Novel Observations. *J. Mol. Catal.* **1994**, *94*, 323−333.
(63) Choung, J. W.; Nam, I. S.; Ham, S. W. Effect of Promoters Including Tungsten and Barium on the Thermal Stability of V2o5/Sulfated Tio2 Catalyst for No Reduction by Nh3. *Catal. Today* **2006**, *111*, 242−247.
(64) Yan, T.; Liu, Q.; Wang, S. H.; Xu, G.; Wu, M. H.; Chen, J. J.; Li, J. H. Promoter Rather Than Inhibitor: Phosphorous Incorporation Accelerates the Activity of V2o5-Wo3/Tio2 Catalyst for Selective Catalytic Reduction of Nox by Nh3 (Vol 10, Pg 2747, 2020). *ACS Catal.* **2020**, *10*, 5602−5602.



https://doi.org/10.1021/acs.jpcc.1c04150
*J. Phys. Chem. C* 2021, 125, 16766−16775